Eur Biophys J (2007) 36:239–252
DOI 10.1007/s00249-006-0124-0

ORIGINAL PAPER

The configuration of the Cu^{2+} binding region in full-length human prion protein

Pablo del Pino · Andreas Weiss · Uwe Bertsch · Christian Renner · Matthias Mentler · Klaus Grantner · Ferdinando Fiorino · Wolfram Meyer-Klaucke · Luis Moroder · Hans A. Kretzschmar · Fritz G. Parak

Received: 20 September 2006 / Revised: 11 December 2006 / Accepted: 18 December 2006 / Published online: 16 January 2007

Abstract The cellular prion protein (PrP^C) is a Cu^{2+} binding protein connected to the outer cell membrane. The molecular features of the Cu^{2+} binding sites have been investigated and characterized by spectroscopic experiments on PrP^C-derived peptides and the recombinant human full-length PrP^C (hPrP-[23-231]). The hPrP-[23-231] was loaded with ^{63}Cu under slightly acidic (pH 6.0) or neutral conditions. The PrP^C/Cu^{2+}-complexes were investigated by extended X-ray absorption fine structure (EXAFS), electron paramagnetic resonance (EPR), and electron nuclear double resonance (ENDOR). For comparison, peptides from the copper-binding octarepeat domain were investigated in different environments. Molecular mechanics computations were used to select sterically possible peptide/Cu^{2+} structures. The simulated EPR, ENDOR, and EXAFS spectra of these structures were compared with our experimental data. For a stoichiometry of two octarepeats per copper the resulting model has a square planar four nitrogen Cu^{2+} coordination. Two nitrogens belong to imidazole rings of histidine residues. Further ligands are two deprotonated backbone amide nitrogens of the adjacent glycine residues and an axial oxygen of a water molecule. Our complex model differs significantly from those previously obtained for shorter peptides. Sequence context, buffer conditions and stoichiometry of copper show marked influence on the configuration of copper binding to PrP^C.

Keywords Electron nuclear double resonance · Electron spin echo envelope modulation · Extended X-ray absorption fine structure spectroscopy · Prion protein · Protein structure

Electronic supplementary material The online version of this article (doi:10.1007/s00249-006-0124-0) contains supplementary material, which is available to authorized users.

P. del Pino · A. Weiss · M. Mentler · K. Grantner · F. G. Parak (✉)
Physics Department E17,
Technical University Munich,
85747 Garching, Germany
e-mail: fritz.parak@ph.tum.de

U. Bertsch · H. A. Kretzschmar
Institute for Neuropathology,
Ludwig-Maximilians-University,
81377 Munich, Germany

C. Renner · F. Fiorino · L. Moroder
Max-Planck Institute for Biochemistry,
Martinsried, Germany

W. Meyer-Klaucke
EMBL c/o DESY, Notkestr. 85,
22603 Hamburg, Germany

Introduction

Transmissible spongiform encephalopathies (TSEs) in mammals are neurodegenerative diseases caused by an infectious agent called prion, which seems to be exclusively composed of the disease-related isoform PrP^{Sc} of the cellular prion protein (PrP^C). Prions represent a kind of infectious particles which differ from other known pathogen agents like bacteria, fungi, parasites, viroids or viruses, both from the structural and pathogenic point of view. Conversion of PrP^C into PrP^{Sc} and deposition of the pathogenic isoform in the central nervous system (CNS) is considered to be the key event in the development of TSEs among which are found diseases such as Bovine spongiform

encephalopathy (BSE) in cattle, scrapie in goats and sheep, and, kuru and Creutzfeldt-Jakob disease (CJD) in humans (Prusiner 1998).

Cellular prion protein is a membrane protein attached through a glycosylphosphatidylinositol (GPI) anchor to the cell surface (Stahl et al. 1987). It is mainly found in neurons within the CNS (Kretzschmar et al. 1986; Moser et al. 1995; Herms et al. 1999). The physiological function(s) of PrP^C remain(s) unclear despite its key roll in the pathogenesis of TSEs. However, there is little doubt about the biological relevance of the copper binding to PrP^C (Brown et al. 1997; Kramer et al. 2001). A number of studies link PrP^C function to its ability to bind Cu^{2+}, playing a role in the copper uptake from extracellular environments to endosomes and the inverse release process (Brown et al. 1997; Pauly and Harris 1988). Moreover, it has been suggested recently that PrP^C reduces Cu^{2+} ions prior to their transfer to Cu^+-specific intracellular trafficking proteins (Miura et al. 2005).

Cellular prion protein binds Cu^{2+} with high affinity in the N-terminal domain of the protein, specifically in the octarepeat region, which consists of four tandem repeats of the sequence PHGGGWGQ (Brown et al. 1997; Kramer et al. 2001). This amino acid sequence motif can bind up to four Cu^{2+} ions and spans the residues 60-91 in human PrP^C. Inherited amplification of the number of octapeptide repeats in mutant forms of PrP^C has been linked to several familial cases of prion human diseases (Skworc et al. 1999; Windl et al. 1996; Nicholl et al. 1995). Therefore, knowledge of the three-dimensional (3D) structure of the N-terminus of PrP^C and particularly of the Cu^{2+}-binding sites may be important for the identification of the physiological function of PrP^C as well as for advanced understanding of the pathological mechanisms of prion diseases. The large flexibility of the unstructured N-terminus has made a complete structure determination by NMR impossible so far. The N-terminus of the prion protein becomes more structured in the presence of Cu^{2+}, but the presence of paramagnetic ion imposes limits to standard NMR structural analysis because of the fast relaxation of the Cu^{2+} ion. Therefore, a variety of other spectroscopic techniques has been applied to investigate the structure of the Cu^{2+}-binding site of the PrP^C which range from crystal structure analysis by X-ray diffraction (Burns et al. 2002), Raman spectroscopy (Miura et al. 1996, 1999, 2005), fluorescence (Stöckel et al. 1998), circular dichroism (CD), (Viles et al. 1999; Burns et al. 2002), extended X-ray absorption fine structure (EXAFS) (Hasnain et al. 2001; Morante et al. 2004; Redecke et al. 2005) to electron paramagnetic resonance (EPR) (Burns et al. 2003) and EPR-derived techniques such as electron nuclear double resonance (ENDOR) (Van Doorslaer et al. 2001; Mentler et al. 2005), electron spin echo envelope modulation (ESEEM) (Burns et al. 2002; Chattopadhyay et al. 2005) or hyperfine sublevel correlation spectroscopy (HYSCORE) (Van Doorslaer et al. 2001; Chattopadhyay et al. 2005). Most spectroscopic investigations addressing the Cu^{2+} binding site of the PrP^C were carried out on PrP^C-derived peptides lacking the C-terminal domain. These studies demonstrated that at full Cu^{2+} occupancy each HGGGW segment within the octarepeat domain binds a single Cu^{2+} ion (Aronoff-Spencer et al. 2000; Burns et al. 2002, 2003). Recent studies from laboratories of Glenn L. Millhauser (Chattopadhyay et al. 2005) on a number of PrP-derived sequences at pH 7.4, have identified and modeled three distinct coordination modes in the octarepeat domain as a function of copper occupancy.

Here we present the results of a combination of EXAFS, EPR and ENDOR measurements together with molecular mechanics calculations. They were performed on the recombinant human prion protein, hPrP-[23-231], isolated from a bacterial expression system. For comparison we also investigated a number of synthetic PrP^C-derived peptides containing amino acid sequences from the octarepeat domain. The results are compared with existing models of the Cu^{2+}-binding site of the octarepeat domain. A novel structural model for the entire octarepeat region of PrP^C in the context of the full-length protein is proposed.

Materials and methods

Peptide synthesis

The pentapeptide, octapeptide and tetraoctapeptide corresponding to the sequences 61-65, 60-67 and 60-91 of $hPrP^C$, respectively, were synthesized in the N-acetylated and C-amidated form to avoid end group effects and thus, to properly mimic this sequence portion in the intact protein as described previously (Renner et al. 2004).

Production of recombinant human PrP-[23-231]

Recombinant PrP-[23-231] was produced and purified essentially as described previously (Giese et al. 2004). Fractions containing purified PrP were pooled, concentrated with a centriprep device and finally diluted 1:50 for refolding into 10 mM MES (pH 6.0). Solutions of refolded PrP were stirred at 4°C for 4–12 h and aggregates removed by centrifugation for 30 min at

17,000 rpm in a Beckmann JA-17 rotor at 4°C. Supernatants were concentrated again using centriprep YM10 ultrafiltration cells and cleared form aggregates by centrifugation at 16,000×*g* for 30 min at 4°C. PrP was finally dialyzed against 2 mM MES (pH 6.0) to remove traces of urea and imidazole. The native fold of purified PrP was confirmed by CD spectroscopy using a Jasco 750 CD-spectrophotometer. Absence of chelators like EDTA and imidazole was confirmed by NMR spectroscopy. Dialyzed PrP solutions of 50–100 μM PrP at pH 6.0 were supplemented with crystaline $^{63}CuCl_2$ to yield a molar ratio of 5:1 of $^{63}Cu^{2+}$ to PrP. Solutions were kept on ice for 1 h then centrifuged for 30 min at 16,000×*g* and 4°C. For the precipitation of PrP/Cu^{2+} complexes under varying pH conditions the supernatants were either supplemented with 100 mM MOPS (pH 7.0) directly before addition of ammonium sulfate or the complexes were directly precipitated by addition of solid ammonium sulfate to a saturation of 90%. Precipitation was performed overnight on ice before the protein was pelleted by centrifugation for 30 min at 16,000×*g* and 4°C.

Sample preparation

^{63}CuO from Chemotrade was stirred in 6 M HCl for 3 h at room temperature. Then the solution was filtered on Millex-GV 0.45 μm and the aqueous layer was lyophilized to yield $^{63}CuCl_2$ in quantitative amounts. Peptide concentrations were determined by weight and peptide content. The pH adjustments were performed by addition of 0.5 M NaOH or 0.5 M HCl and equilibration of the solutions for 24 h. Protein concentrations of PrP were determined by absorption measurements at 280 nm. An extinction coefficient of 56,590 M^{-1} cm^{-1} was used for calculation of the protein concentration. Samples of 1 mM pentapeptide and octapeptide and its 1:1 complex with Cu^{2+} were prepared in 25 mM *N*-ethyl-morpholine (NEM), 150 mM KCl and 20% glycerol. Samples of recombinant hPrP-[23-231] and tetraoctapeptide were prepared in different buffer systems. Cu^{2+} contents were varied within each kind of buffer preparation as follows: *Buffer a and b:* Pellets of the recombinant human PrP-[23-231] were resuspended in minimal volumes of either 10 mM MES (pH 6.0) (buffer *a*) or 10 mM MOPS (pH 7.0) (buffer *b*) and transferred into appropriate sample holders for EPR or EXAFS measurements. We also prepared a soluble hPrP/^{63}Cu complex as follows: hPrP at a concentration of 0.7 mM was mixed in buffer *a* at pH 6.0 with $^{63}CuCl_2$-solution of pH 6.0 at a molar ratio of 1:5 of hPrP to $^{63}Cu^{2+}$. The solution was kept on ice for 1 h then centrifuged for 30 min at 16,000×*g* and 4°C. The supernatant was dialyzed exhaustively against 2 mM MES at pH 6.0. The remaining copper concentration in the dialyzed sample was determined by inductively coupled plasma mass spectroscopy (ICP-MS). *Buffer c*: Samples of 0.80 or 0.35 mM tetraoctapeptide coordinated with 1, 2, or 3 Cu^{2+} equivalents were prepared in 100 mM ammonium acetate buffer containing DPC-d_{38} (Eurisotop, France) at a peptide/detergent ratio of 1:100. *Buffer d*: Samples of 0.106 mM tetraoctapeptide coordinated with 1, 2, 3, or 4 Cu^{2+} equivalents were prepared in 25 mM NEM, 150 mM KCl and 20% glycerol. *Buffer e*: Samples of 0.35 mM tetraoctapeptide complexes with 1, 2, 3, or 4 Cu^{2+} equivalents were prepared in 10 mM phosphate buffer containing 35 mM DPC-d_{38} (Eurisotop, France) resulting in a peptide/detergent ratio of 1:100. The buffers and the pH-values of the samples are summarized in Table 1.

Determination of copper concentrations

Inductively coupled plasma mass spectroscopy on diluted samples was done on a Elan 6100 mass

Table 1 All samples of this study. Amount of Cu^{2+}, pH values, buffer and applied spectroscopic methods are specified for each sample

Sample	Peptide	Cu^{2+}equivalent	Buffer	pH	EPR	ENDOR	EXAFS
Recombinant hPrP (A)	hPrP 23-231	1.7	*a*	6.0	✓	–	✓
Recombinant hPrP (B)	hPrP 23-231	2.7	*b*	7.0	✓	✓	✓
Tetraoctapeptide (C)	hPrP 60-91	1.0	*c*	7.5	✓	✓	–
Tetraoctapeptide (C)	hPrP 60-91	2.0–3.0	*c*	7.5	✓	–	–
Octapeptide (D)	hPrP60-67	1.0	*d*	7.1	✓	✓	✓
Pentapeptide (E)	hPrP 61-65	1.0	*d*	7.5	✓	✓	–
Tetraoctapeptide (F)	hPrP 60-91	1.0–4.0	*d*	7.5	✓	–	–
Tetraoctapeptide (G)	hPrP 60-91	1.0–4.0	*e*	7.5	✓	–	–
Recombinant hPrP (H)	hPrP 23-231	1.3	*a*	6.0	–	–	✓

The different buffers are identified by letters *a* to *e*, where *a*: 10 mM 2-morpholinoethanesulfonic acid (MES); *b*: 10 mM 3-*N*-morpholinopropanesulfonic acid (MOPS); *c*: 100 mM ammonium acetate buffer containing dodecylphosphocholine (DPC) micelles at a peptide/detergent ratio of 1:100; *d*: 25 mM *N*-ethyl-morpholine (NEM), 150 mM KCl, 20 % glycerol; *e*: 10 mM sodium phosphate buffer containing DPC micelles at a peptide/detergent ratio of 1:100

spectrometer (Perkin-Elmer, Sciex, Toronto, Canada) with external calibration by multi-element stndards (Merck, Darmstadt, Germany) and an internal ^{103}Rh standard (final concentration 10 μg/l). The mass spectrometer combined with a conventional cross flow nebulizer, a peristaltic pump for sample introduction, and an AS-90plus autosampler (Perkin-Elmer), an Rf power of 1,200 W, a sample uptake of 1 ml/min and wash time of 80 s after each sample, a nebulizer gas flow of 0.9 l/min, and a dwell time per mass of 80 ms with 50 scans per sample and 5 replicates were employed for the simultaneous detection of ^{63}Cu, ^{65}Cu, ^{55}Mn, ^{57}Fe, and ^{66}Zn isotopes. One should note here, that only for the soluble hPrP[23-231] copper complex a direct measurement of the copper content was possible (ICP-MS gave a value of 1.3 Cu^{2+} per hPrP). For the precipitated samples, however, the amount of copper in the pellets has to be calculated by subtraction of the concentration measured for the supernatant from that of the entire samples before precipitation. Especially at pH 7.0, where unbound copper precipitates as copper hydroxide, a certain amount of precipitated copper hydroxide can be carried over into the sample. Therefore the obtained values (1.7 and 2.7 Cu^{2+} per hPrP) are upper limits.

EPR and ENDOR measurements

A Bruker ELEXSYS 580 X-band spectrometer with an Oxford cryostat with variable temperature control was used for all measurements. Continuous wave EPR spectra were taken at 77 K with a modulation amplitude of 3 Gauss and a microwave power of 0.6346 mW in a T_{102} Bruker cavity. The program package Xemr was used to simulate EPR spectra (compare: http://www.epr.chem.jyu.fi/xemr/). ENDOR spectra were recorded at 17 K. The microwave power was 20.0195 mW, the radio frequency power was 1 dB at a maximum power output of 500 W and radio frequency modulation amplitude of 300 kHz. Several different magnetic fields $\vec{B}$ were used as working points to select different orientations of the molecules (compare Table 2). A home-made program was used to evaluate the ENDOR spectra. For details see (Mentler et al. 2005).

The EPR spectra of the samples studied show the typical features of square-planar type 2 Cu^{2+} complexes where three of the four hyperfine transitions in the parallel region of the spectra (low-field range) are apparent while the fourth is masked by overlap with the hyperfine transitions in the perpendicular region towards the high-field region. Figure 1 shows the geometry used for the analysis of our EPR and ENDOR spectra. The EPR spectra are determined by

Table 2 Electron nuclear double resonance (ENDOR) investigations of the four samples shown in Fig. 5

Working point	Magnetic field (mT)	θ selection species I (°)	θ selection species II (°)
1	279.0	0	25
2	286.4	27	32
3	293.8	0, 40	21, 48
4	301.0	31, 50	38, 57
5	308.2	0, 45, 59	10, 51, 65
6	315.6	35, 58, 69	38, 63, 74
7	323.0	0, 54, 72, 80	58, 79, 85
8	328.3	34, 70, 90	29, 87
9	334.0	66	63

The table gives the correlation of the working points with the magnetic fields of the EPR spectrometer. For each working point only molecules contribute which have a certain orientation θ to the magnetic field, where θ defines the angle formed between the applied magnetic field and the z-axis of the molecular coordinate system (see Fig. 1)

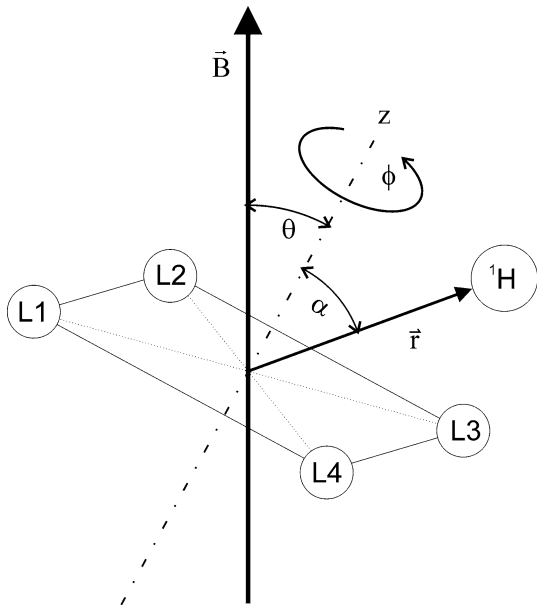

Fig. 1 Coordinate system used for calculations. The four ligands L1–L4 of the Cu^{2+} define a plane. The normal of this plane is called z and rotations around this axis are described by the angle ϕ. The hydrogen atom H at the position $\vec{r}$ forms an angle α with respect to z. The applied magnetic field $\vec{B}$ is rotated by an angle θ with respect to z

the interaction of the $^{63}Cu^{2+}$ spin ($S = 1/2$) with the magnetic field, the nuclear spin of ^{63}Cu ($I = 3/2$), and the nuclear spin of ^{14}N ligands ($I = 1$), which reflects essentially the interaction of the Cu^{2+} with the first coordination shell. The Hamiltonian becomes:

$$\hat{H} = \beta_e \hat{S} \overleftrightarrow{g} \vec{B} + \hat{S} \overleftrightarrow{A}^{Cu} \hat{I}^{Cu} + \hat{S} \overleftrightarrow{A}^{N} \hat{I}^{N} \quad (1)$$

where the terms represent the electron Zeeman interaction, the nuclear hyperfine interaction of the $^{63}Cu^{2+}$,

and the nuclear superhyperfine (SHF) interaction of ^{14}N respectively. ß$_e$ is the Bohr magneton, $\hat{S}$, $\hat{I}^{Cu}$, are electron and nuclear spin operators of the Cu^{2+} and the ^{14}N, respectively. The $\vec{g}$ tensor and the magnetic hyperfine tensor $\vec{A}$ are defined as usual (see e.g. Hurst et al. 1985).

The hyperfine parameters of protons can be determined by ENDOR. The interaction can be described by the Hamiltonian:

$$\hat{H}_H = g_N \beta_N B \hat{I} + \hat{S} \overleftrightarrow{A}^{Dipole} \hat{I}. \quad (2)$$

The first term is the nuclear Zeeman energy, the second term describes the hyperfine interactions of the nuclear spin $\hat{I}$ of the hydrogens with the electron spin S of the copper atom. The isotropic Fermi interaction and the nuclear quadrupole interactions where neglected in our evaluation. g_N is the nuclear g-factor, β_N is the nuclear magneton, $\hat{I}$ is the nuclear spin operator, and A^{Dipole} the dipole–dipole interaction matrix. In principle ENDOR is also sensitive to the hyperfine interaction with ^{14}N ($I = 1$). However, we were unable to resolve these signals. For a more detailed description see (Mentler et al. 2005).

EXAFS measurements

Extended X-ray absorption fine structure experiments were performed with synchrotron radiation at the European molecular biology laboratory (EMBL) beam line D2 at Deutsches elektronen synchrotron (DESY). The storage ring DORIS was operating at an energy of 4.5 GeV with a positron current between 90 and 145 mA. A Si(111) double monochromator with focusing mirrors selected energies around the Cu-K_α edge. Bragg-reflections of a Si-crystal were used for the energy calibration (Pettifer and Hermes 1985). The measurements were performed at 35 K. A Canberra 13-element fluorescence detector was used to collect the copper K_α-fluorescence. The total measuring time was divided into several scans taking between 30 and 45 min. The standard procedures of the EMBL were used for the data reduction (Nolting and Hermes 1992). The k^3-weighted Cu^{2+} EXAFS spectra $\chi(k)$ were refined with software package EXCURV 9.262 (Binsted et al. 1992). Phase shifts and scattering amplitudes were computed according to (Rehr and Albers 1990).

Molecular mechanics and simulated annealing

Modeling calculations were performed to obtain structures with low energy and good covalent geometry. The classical molecular mechanics force field CHARMM22 (MacKerell et al. 1998) and additional MM parameters (Mentler et al. 2005) derived by density functional theory (DFT) calculations using the BP86 functional and the 6-31G* basis set provided by the program Gaussian 98 (Frisch 1998) were used for model building. Standard simulated annealing protocols within the program XPLOR (Brünger 1992) were used for the molecular dynamics simulations.

Results

Electron paramagnetic resonance

Figure 2 shows the EPR spectra of recombinant human PrP-[23-231] with different Cu^{2+} contents. There are four possible binding places within the tetraocta-repeat region. For comparison are also given: the spectra of the tetraoctapeptide PrP-[60-91] (four possible Cu^{2+} binding places), the single octapeptide PrP-[60-67] (one possible Cu^{2+} binding place) and the pentapeptides PrP-[61-65] (one possible Cu^{2+} binding place). All spectra show the typical features of square–planar copper complexes. The hyperfine pattern reveals distinct species. The pentapeptide/Cu^{2+} at pH 7.5 and the octapeptide/Cu^{2+} complexes show the same pattern. We attribute this type of EPR spectra to a configuration called species I. From previous studies of our laboratory (Mentler et al. 2005) and X-ray diffraction studies (Burns et al. 2002) the Cu^{2+} coordination geometry of species I is well known. The EPR spectra of PrP-[60-91]/1 Cu^{2+} and the recombinant hPrP-[23-231] samples, differ clearly from species I spectra and are therefore attributed to a species II (compare Table 3). The existence of different species I and II can also be seen from the high field region of the EPR spectra (Fig. 3). The species II samples, hPrP-[23-231] and the tetraoctapeptide PrP-[60-91]/1 Cu^{2+}, share the same SHF pattern while the isolated octarepeat, species I has a different splitting. Based on these evidences, we can assume two different configurations for our species I and II samples. The appearance of species I and II can depend on the environment and the Cu^{2+} load as demonstrated for tetraoctapeptides (compare Fig. 4). At several conditions we find mixtures of molecules belonging to species I and II, such spectra are shown mainly to demonstrate the difficulty of a comparison of different studies as subtle changes of the environment can lead to very different results. However, it is evident that tetraoctapeptide samples loaded with 1 Cu^{2+} equivalent exhibit species II, independent of the buffer system.

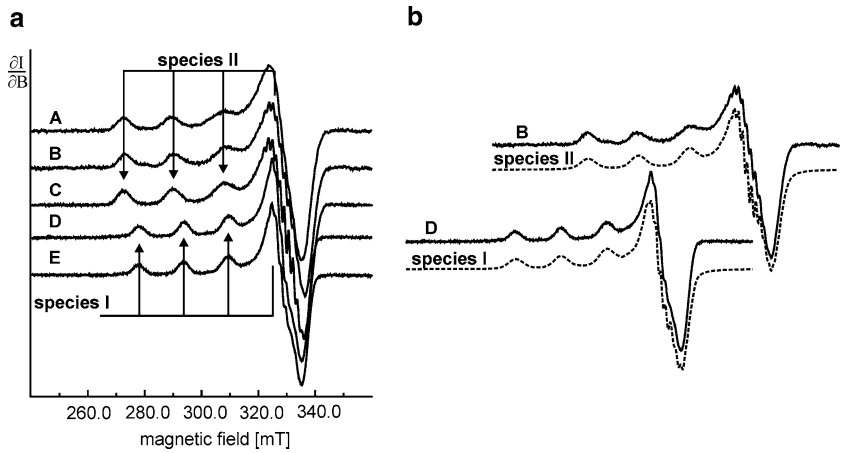

Fig. 2 **a** X-band spectra of recombinant hPrP with Cu^{2+} and Cu^{2+} loaded peptides. (*A*) hPrP-[23-231] at pH 6.0 with 1.7 Cu^{2+} equivalents; (*B*) hPrP-[23-231] at pH 7.0 with 2.7 Cu^{2+} equivalents; (*C*) hPrP-[60-91] in ammonium acetate buffer plus DPC micelles at pH 7.5 with 1 Cu^{2+} equivalent; (*D*) octapeptide at pH 7.5 with 1 Cu^{2+} equivalent, (*E*) pentapeptide at pH 7.5 with 1 Cu^{2+} equivalent. **b** X-band spectra of samples B and D and simulated spectra (*dotted lines*) for these samples. Electron paramagnetic resonance (EPR) parameters for these simulations are shown in Table 3

Table 3 Parameters of the simulated EPR spectra, where g_{xx}, g_{yy}, g_{zz} are the principal values of the $\vec{g}$ tensor, $A^{Cu}_{xx}, A^{Cu}_{yy}, A^{Cu}_{zz}$ are the principal values of the magnetic hyperfine $\overleftrightarrow{A}^{Cu}$ tensor, and $A^{N}_{xx}, A^{N}_{yy}, A^{N}_{zz}$ are the principal values of the magnetic superhyperfine $\overleftrightarrow{A}^{14N}$ tensor (compare Eqs. 1 and 2)

Simulation	$(g_{xx}\ \ g_{yy}\ \ g_{zz})$	$\left(A^{Cu}_{xx}\ \ A^{Cu}_{yy}\ \ A^{Cu}_{zz}\right)$[mT]	$\left(A^{N}_{xx}\ \ A^{N}_{yy}\ \ A^{N}_{zz}\right)$[mT]	Coordination
Species I	(2.065 2.070 2.249)	(9.6 10.7 170.0)	(15.4 15.4 12.6)	3N–1O
Species II	(2.074 2.055 2.264)	(10.0 14.0 189.0)	(14.5 14.5 14.0)	4N

ENDOR

In order to investigate the ^1H positions in the Cu^{2+} complexes, ENDOR spectra were recorded at nine different magnetic fields $\vec{B}$ for four samples representative of both species. Table 2 shows the orientations of the selected molecules for the studied samples. The corresponding ENDOR spectra are depicted in Fig. 5. They show ^1H resonances in the region of 9–17 MHz which appear symmetrically around the proton nuclear Zeeman frequency of 12–14 MHz. A comparison indicates that the ^1H-environment in all the investigated samples is qualitatively very similar. However, the spectra of the species I Cu^{2+} complexes, pentapeptide and octapeptide, have a different distribution of intensities than the species II complexes, represented by the tetraoctapeptide and the recombinant hPrP-[23-231] loaded with 2.7 Cu^{2+} equivalents.

EXAFS measurements

Figure 6a displays the k^3-weighted EXAFS spectra for the octapeptide and the hPrP-[23-231] samples and Fig. 6b their Fourier transformed. In agreement with the results of EPR and ENDOR two different EXAFS patterns are distinguishable. The octapeptide complex species I shows an EXAFS signal which differs from that of the three hPrP-[23-231] complexes belonging to species II. The three species II complexes are very similar, independent of the pH variation and of the precipitation. For hPrP-[23-231]/1.3 Cu^{2+}, in solution at pH 6.0, the statistics is significantly worse compared to the other spectra, due to the lower concentration of peptide/Cu^{2+} complexes. Therefore, samples with precipitated material were measured. The Fourier transformed in Fig. 6b shows the distance of scattering atoms to the absorbing centre as a radial distribution function. The prominent peaks at about 3 and 4 Å can only be explained by multiple scattering processes. They are typical for multiple scattering by imidazole rings. Note, that the intensity of these peaks is much larger in species II than in species I.

Model building and molecular mechanics simulations

Electron paramagnetic resonance measurements are very sensitive to changes in the ligand environment around the Cu^{2+} ion. With our measurements we could

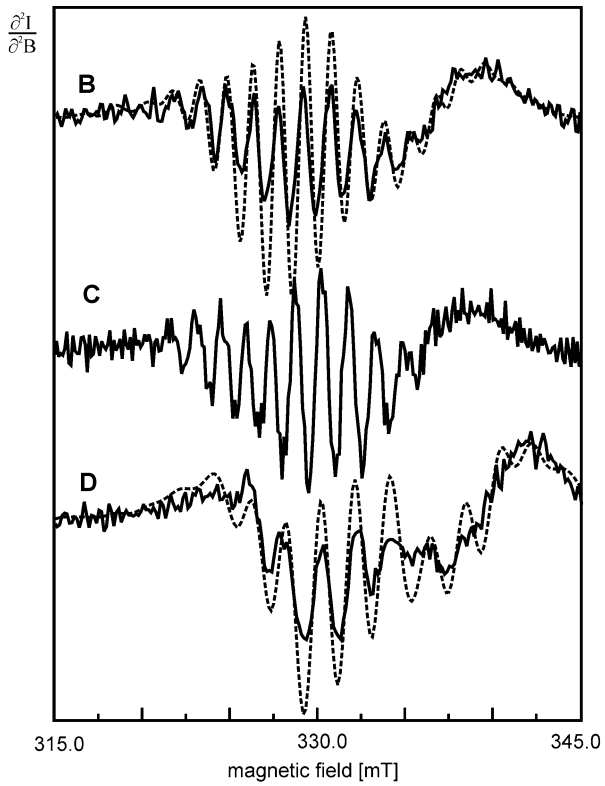

Fig. 3 EPR second derivatives of the high field region of spectra shown in Fig. 2. *B* hPrP-[23-231] at pH 7.0 with 2.7 Cu^{2+} equivalents, *dotted line* is a simulation of EPR spectrum for species II; *C* PrP-[60-91] in ammonium acetate buffer containing DPC at pH 7.5 with 1 Cu^{2+} equivalent; *D* octapeptide at pH 7.5, *dotted line* is a simulation of EPR spectrum for species I. Parameters for EPR simulations are given in Table 3

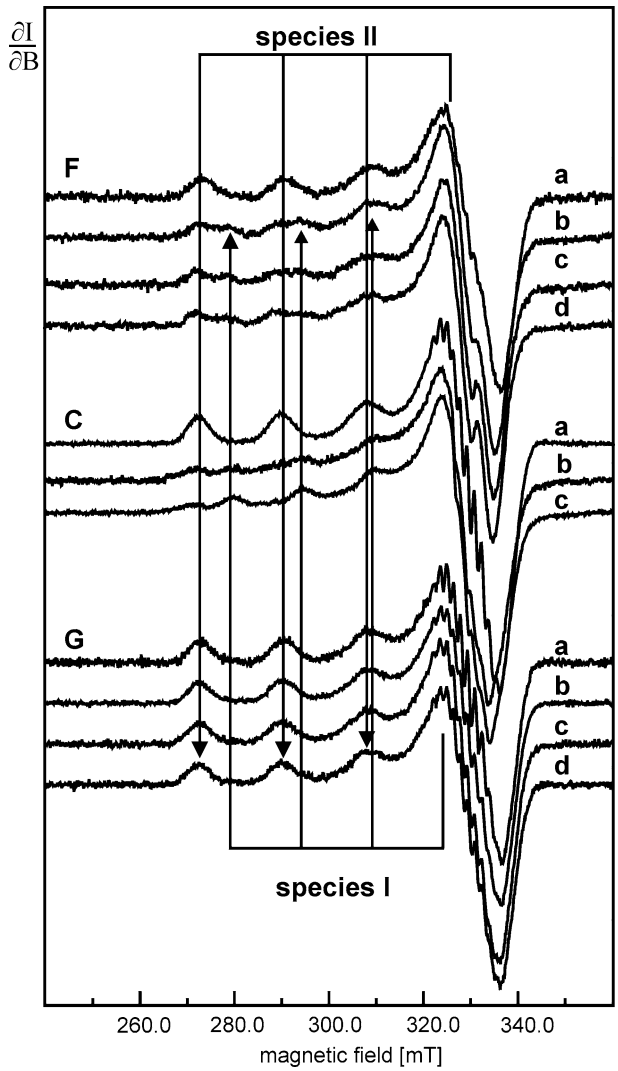

Fig. 4 EPR spectra of tetraoctarepeat peptides, PrP-[60-91] in different buffer systems and Cu^{2+} equivalents. *Group F* NEM buffer; *group C* ammonium acetate buffer containing DPC; *group G* sodium phosphate containing DPC. Within the groups: different Cu^{2+} equivalents (1 Cu^{2+}, 2 Cu^{2+}, 3 Cu^{2+}, and 4 Cu^{2+})

identify two different Cu^{2+} environments. Species I is well known from the isolated octarepeat (Burns et al. 2002; Mentler et al. 2005). It is characterized by a planar copper complex with three nitrogen and one oxygen ligands as well as an axial oxygen from a water molecule. One of the nitrogen atoms is the N_δ of the histidine. With this coordination the EPR spectra (Fig. 2) and especially the high field region can be simulated (Fig. 3). In principle, the Peisach–Blumberg correlations (Peisach and Blumberg 1974) connect hyperfine parameters with the type of Cu^{2+} ligands. Unfortunately, the information is ambiguous in the present case. However, in Cu^{2+} complexes, nitrogen ligands can interact with the unpaired electron of Cu^{2+} and give rise to further splitting of the hyperfine pattern, called SHF interaction. The multiplicity of the lines in the SHF structure accounts for the number of nitrogen ligands. Figure 3 highlights the SHF structure for species I and II in the high-field region of the EPR spectra. The splitting of the SHF lines in both species II and I, is about 1.5 mT, which is in agreement with previously reported SHF splitting values for nitrogen coordination in Cu^{2+} complexes (Scholl and Hüttermann 1992; Lemos et al. 2000; Yuan et al. 1999; Katterle et al. 2002). The increase of the SHF lines from species I to species II strongly indicates an increase of the nitrogen ligands from 3 to 4. Planar coordinations with 4 N for species II and 3 N for species I give good theoretical simulated spectra (compare Figs. 2, 3). The SHF parameters used for the EPR simulations are in agreement with the literature (Scholl and Hüttermann 1992; Yuan et al. 1999). The relatively small line widths and the good agreement with the simulated spectrum lead to the conclusion that each sample contains essentially one species, either I or II.

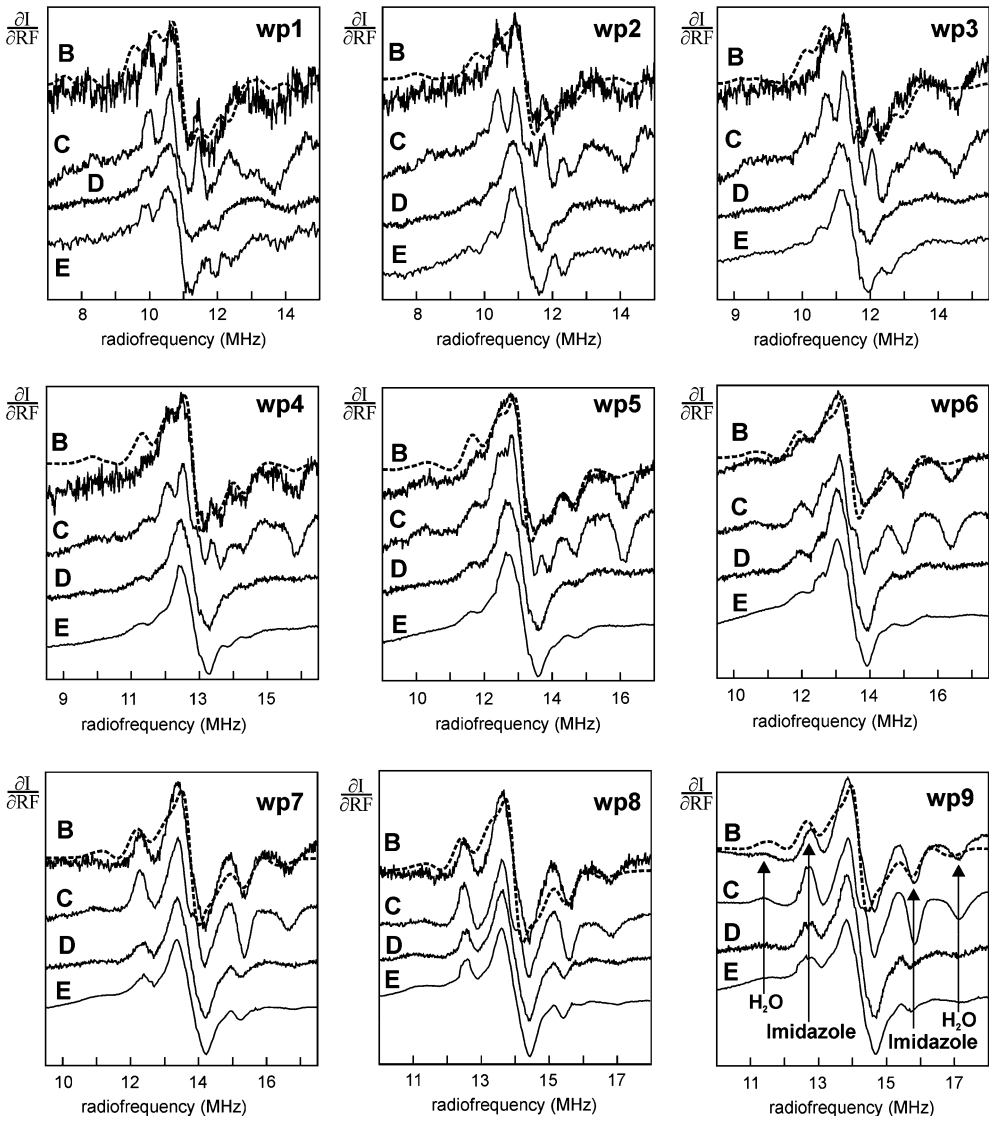

Fig. 5 Electron nuclear double resonance (ENDOR) spectra of hPrP-[23-231], (*B*) at pH 7.0 loaded with 2.7 Cu^{2+} equivalents *C* tetraoctapeptide at pH 7.5 in ammonium acetate buffer containing DPC, *D* Cu^{2+} loaded octapeptide, and *E* pentapeptide. The spectra were taken at nine different magnetic fields (wp1 to wp9). The *dotted line* gives the ENDOR spectrum calculated with the final model for the recombinant hPrP. *Arrows* point at resonances expected to stem from imidazole and water hydrogen

The ENDOR analysis reveals a similar ^1H environment of the Cu^{2+}-complexes for species I and II, although according to the EPR data they differ in the number of coordinating nitrogens. This apparent contradiction can be solved if one assumes different imidazole coordination: Species II is ligated to two imidazole nitrogens. This interpretation is supported by the fact that the main intensity differences of the ENDOR spectra are found at resonances expected to stem from imidazole hydrogens (see arrows in Fig. 5). In previous investigations of a species I sample (Mentler et al. 2005), ^1H-resonances were associated to axial water by means of comparison with a deuterated sample. These resonances are also found in ENDOR spectra of the PrP-[60-91]/Cu^{2+} and the hPrP-[23-231]/2.7 Cu^{2+} complexes (see arrows in Fig. 5). Therefore, in species II the Cu^{2+} is coordinated by an axial water molecule, too.

The EXAFS data give another strong support for the ligation of the Cu^{2+} by two histidyl imidazoles. The peaks at about 3 and 4 Å in Fig. 6b are the signatures of histidine ligands (Arnesano et al. 2003a, b; Hasnain et al. 2001). The amplitude of these peaks is enlarged in species II.

With this information at hand, a model of the full-length hPrP-[23-231] ligated with two Cu^{2+} was built, taking into account the similarity of ENDOR spectra of species I and II and four nitrogens ligated to each Cu^{2+}. In our model the nitrogens of the deprotonated amides Gly70, Gly71 and the N_δ of the imidazole of His69 are ligands in species II as well as in species I. However, the oxygen of Gly71 in species I is replaced by the N_δ of His61. An axial water molecule completes the penta coordination. The second Cu^{2+} ion is bound by the third and fourth histidine imidazoles and the corresponding glycines. In this context, one should

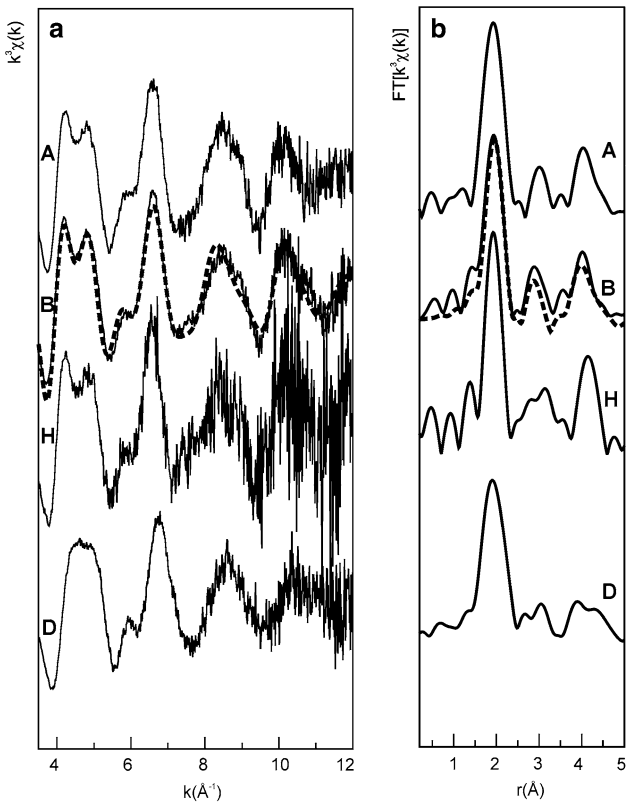

Fig. 6 Extended X-ray absorption fine structure (EXAFS) spectra recorded for the Cu^{2+} loaded complexes. (*A*) hPrP-[23-231] at pH 6.0 with 1.7 Cu^{2+} equivalents precipitated; (*B*) at pH 7.0, precipitated with 2.7 Cu^{2+} equivalents; (*H*) with 1.3 Cu^{2+} equivalents in solution; (*D*) octapeptide/Cu^{2+} at pH 7.1; the *dotted line* is calculated for our final model of the recombinant hPrP

remember that each histidine is a possible Cu^{2+} binding place. Since in the case discussed here one Cu^{2+} coordinates to two histidines, there remain only two binding places which are identical with respect to the first coordination shell. A simplified drawing of one of the two copper binding sites is shown in Fig. 7.

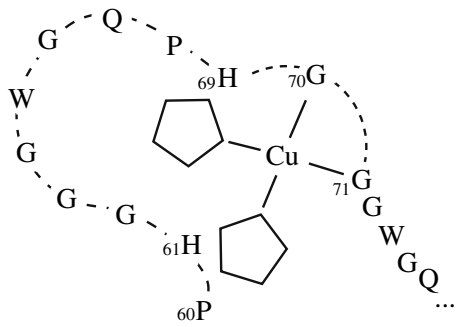

Fig. 7 Sketch of the coordination of Cu^{2+} in the recombinant hPrP in our model

In order to obtain a 3D structure, we employed molecular modeling. For a starting point an extended random coil structure was generated for the peptide and the metal ion was covalently attached to the N_δ of His69 and His85. A water molecule served as a weak axial ligand. A recently developed simulated annealing protocol described in (Mentler et al. 2005) was applied involving cooling from 3,000 to 300 K while switching slowly from a solely ionic Cu^{2+} interaction to a covalently bound Cu^{2+} ion. The MD simulations were carried out using the MM–MD program XPLOR (Brünger et al. 1987) and the CHARMM22 force field. Subsequently these prototypes of models were used to generate 5,000 conformations using the complete MM force field for such copper complexes (Mentler et al. 2005), standard simulated annealing procedures (Brünger et al. 1987) and energy minimization. Selection rules have been applied to reduce the number of structures to 100 by removing all structures which were completely incompatible with the experimental data (e.g. distances of ligands) or with the force field. For the remaining 100 structures EXAFS spectra were calculated taking into account multiple scattering up to five scattering processes. The positions of atoms within the second and third coordination spheres around the copper strongly influence the calculated multiple scattering signal. Therefore, the comparison of calculated EXAFS spectra with experimental data can be used to rule out incompatible conformations. Five conformations with the best EXAFS spectra were selected for further refinement. After choosing a random velocity distribution representing a 400 K ensemble, a short 100 ps MD run subsequently followed by an energy minimization was carried out and 5 times 100 structures were produced. The selection rules described above were applied again and the 50 conformations with the best fit concerning EXAFS spectra were chosen to determine hydrogen positions with respect to the copper centers and to calculate ENDOR spectra. The final model shown in Fig. 8 is in best agreement with all spectroscopic data without violating standard bond lengths or angles.

Discussion

It has to be emphasized that the investigation of species II was essentially performed on the recombinant hPrP-[23-231] in complex with $^{63}Cu^{2+}$. These samples were only partially loaded with Cu^{2+}. Our investigation of full-length hPrP-[23-231] was complicated by the low solubility at neutral and slightly basic pH, where Cu^{2+}-binding to PrP is optimal. Cu^{2+} loading at pH 6.0

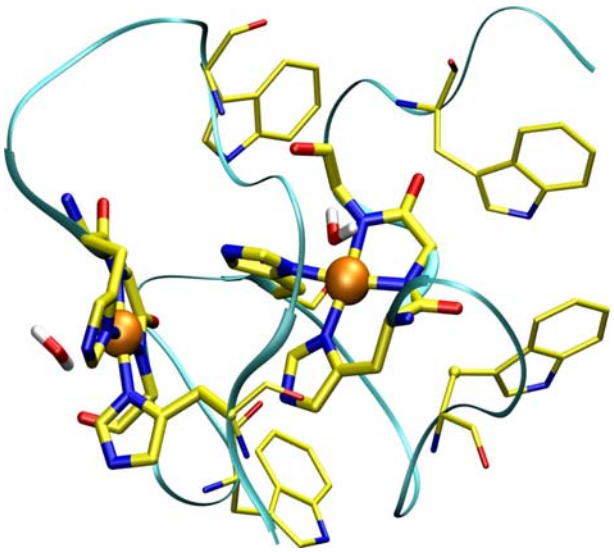

Fig. 8 Representation of the final model. We accentuated the parts of the protein within a radius of 5 Å around the copper centers which were used to simulate and validate our EXAFS, EPR and ENDOR experimental data

followed by precipitation using ammonium sulfate yielded samples with a good signal to background ratio. To get an idea of the intactness of the peptide-Cu^{2+} fold after precipitation, we recorded an EXAFS spectrum of the hPrP-[23-231]/1.3 Cu^{2+} complex in solution at pH 6.0. Within the limits of error bars, because of its lower signal-to-noise ratio, this spectrum shows the same features as the spectra from precipitated samples. There was no hint for any interference of the precipitation procedure with the structure of the copper binding site.

Let us come back to the possible Cu^{2+} sites. It is generally believed that each histidine of the tetraoctarepeat part can bind one Cu^{2+} (Chattopadhyay et al. 2005). Moreover, there is some evidence that a fifth Cu^{2+} can bind in the region between the octarepeat domain and the structured C-terminal part of PrP. Histidine residues corresponding to the positions 96 and 111 of recombinant hPrP(23-231) have been considered as possible binding sites for the fifth Cu^{2+} (Burns et al. 2003). In hPrP-[23-231] we found no evidence that the histidines at position 96 and 111 bind Cu^{2+}. In our model one Cu^{2+} coordinates to two histidines of two octarepeats. This means that we can only bind two Cu^{2+} ions in the octarepeat region. Although the EPR spectra of the of the hPrP-[23-231] loaded with 1.7 and 2.7 Cu^{2+} equivalents represent essentially species II, a contribution of species I cannot be excluded. In principle, we could have a mixture of molecules ligated with 0, 1, 2, 3, and 4 Cu^{2+} where the contributions have a different weight. The sample with 1.7 Cu^{2+} equivalents probably contains molecules with 1 or 2 species II type copper sites occupied. This is endorsed by the fact that a tetraoctapeptide coordinated with one Cu^{2+} shows also a species II type spectrum. For the discussion of the PrP sample with 2.7 Cu^{2+} equivalents one has to have in mind that a tetraoctapeptide with four Cu^{2+} equivalents show a species I spectrum (Burns et al. 2003). In order to bind the 2.7 Cu^{2+} equivalents to PrP the simplest way is to assume an equilibrium of 65% species II (two sites occupied) and 35% species I (four sites occupied).

Simulations with different species I concentrations are given in electronic supplementary material (S1). A contribution of 35% molecules binding as species I is not compatible with the EPR signal. The EPR estimations in S1 indicate that the signal of species I type complexes should be less than 20%. EXAFS simulations with the same percentage of species I and II used for EPR are also in agreement with our experimental data (not shown). At this point the Cu^{2+}-balance is still not even. However, the 2.7 Cu^{2+} equivalent is an upper limit because it is the result of an indirect measurement (see ''Materials and methods'') and we cannot exclude the presence of copper hydroxide precipitate which is EPR silent and therefore invisible in EPR and ENDOR. Simulations of EXAFS spectra with different copper hydroxide amounts, as shown in electronic supplementary material (S2), reveal that we cannot exclude a contribution of up to 0.25 (out of 2.7) equivalents of copper hydroxide that makes no significant change of the EXAFS simulation.

The simulated ENDOR spectrum for the proposed model is a superposition of the spectra of 34 single protons that can be found in less than 5 Å around the two copper ions. For EPR, the two binding sites are identical, since EPR signals are essentially sensitive only to the first coordination shell. However, this is not true for ENDOR because of the different sequence context of the binding site 1 and 2. To illustrate the contribution to the spectrum of the two copper sites we show in Fig. 9 simulations of site 1 and 2 separately together with the sum of both sites and the experimental data from Fig. 5. Detailed information about proton positions is given in electronic supplementary material (S3). The two copper ions shown in our model are 7.8 Å apart. We did not find evidence of dipolar coupling neither in the forbidden nor in the allowed transition region.

The structure of the Cu^{2+} binding region of PrP^{C} was investigated by several groups. Especially the partially Cu^{2+}-saturated octarepeat region found large interest. A comparison of the different findings is limited by the fact that the investigated samples are not

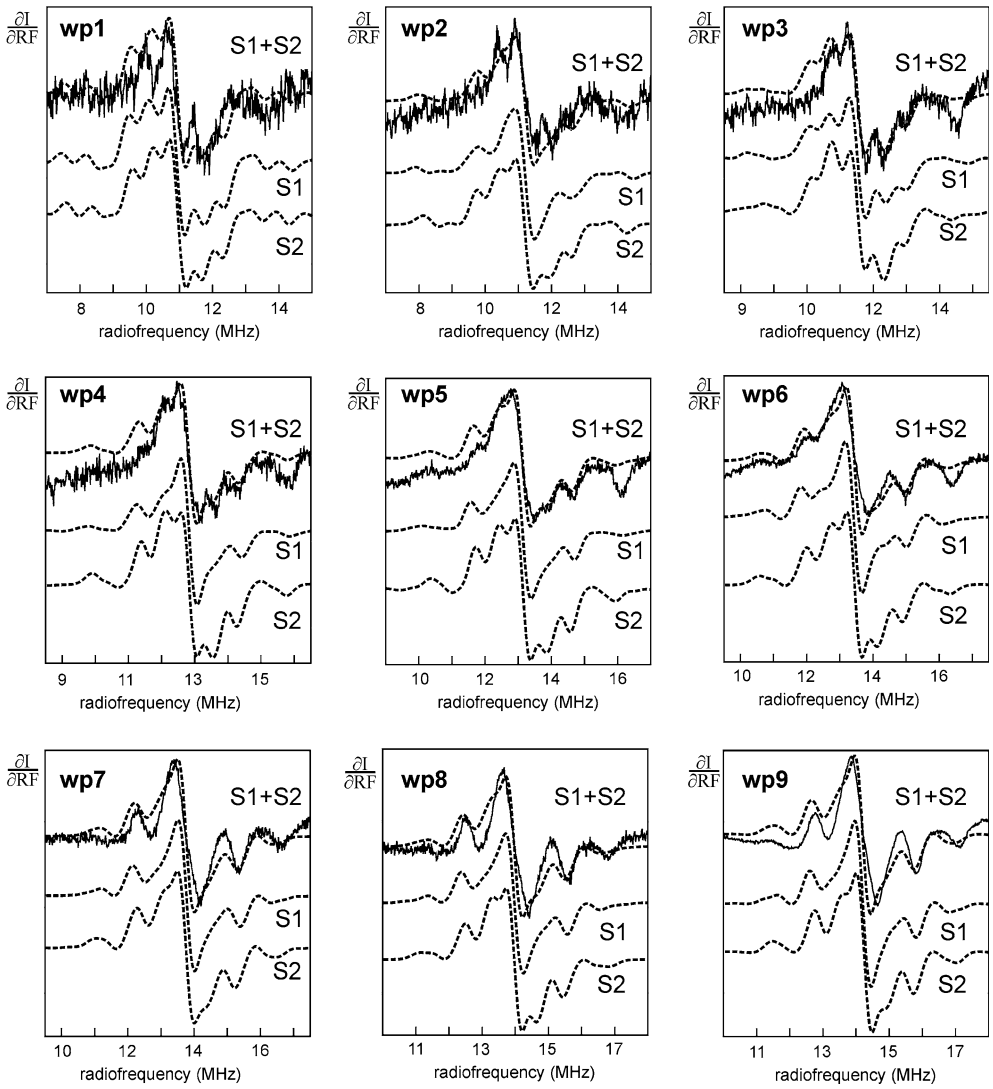

Fig. 9 ENDOR spectra of hPrP-[23-231] at pH 7.0 loaded with 2.7 Cu^{2+} equivalents. The *dotted lines S1* and *S2* are the ENDOR simulations taking into account only protons in a 5 Å radius around copper site 1 and 2, respectively. The *dotted line S1 + S2* is the sum of these two simulations and gives the ENDOR spectrum calculated for the final model for the recombinant hPrP

precisely identical. Stöckel et al. (1998) studied the recombinant Syrian hamster prion protein SHaPrP-[29-231] and various PrP^C fragments at pH 6.0, by means of fluorescence and CD spectroscopies. This early work suggested that SHaPrP-[29-231] binds two Cu^{2+} ions at pH 6.0. Two octarepeat peptides were involved in the binding of each Cu^{2+}. The coordination is effected by a 2N–2O square planar geometry which is formed by one histidyl imidazole nitrogen and one glycine carbonyl oxygen of two adjacent octapeptide repeats each. The glycine carbonyl oxygen in the middle of the glycine triplet in the octarepeat peptide was chosen because this enabled the Trp residue to come into proximity with the Cu^{2+} center, thus explaining the quenching of Trp fluorescence upon binding of Cu^{2+} to SHaPrP-[29-231]. The number of bound Cu^{2+}-ions and the formation of the Cu^{2+} binding site by two His and two Gly residues is in agreement with our results. However, in our model the glycine carbonyl oxygens are replaced by amid nitrogens.

Viles et al. (1999) studied the Cu^{2+} binding site of PrP^C-derived peptides fragments corresponding to 2-, 3- and 4-octarepeat sequences by using visible absorption-, CD- and EPR-spectroscopy. The peptide PrP-[58-91] was studied by X-band EPR with one, two and three equivalents of Cu^{2+}. The spectra are practically the same as those in this communication showing the species II. However, different Cu^{2+} coordinations were proposed. In the square planar 3N–1O geometry the oxygen stems from a water molecule which is in contradiction to our ENDOR results. Although we also claim the coordination of the Cu^{2+} with two histidines there is a contrast to our model. Viles et al. (1999) propose that each histidine represents a link between two Cu^{2+} ions binding with N_δ and N_ε to Cu^{2+}

ions in successive octapeptides. In our case only N_δ participates in the binding.

Morante et al. (2004) studied the Cu^{2+} binding site of the αBoPrP-[24-242] using XAS spectroscopy. Note that the BoPrP has six octapeptide repeats within its octarepeat domain. They found that the Cu^{2+} binding site in αBoPrP-[24-242] at half-site Cu^{2+} occupancy consists of pentacoordinated Cu^{2+} sites with one axially bound water molecule and two equatorial nitrogen atoms from two histidyl imidazole rings. The remaining two equatorial ligands could not be determined unambiguously by this XAS study. As possible candidates amid nitrogen or carbonyl oxygen atoms from glycine residues were considered. In the present study, we were able to resolve unambiguously the uncertainty regarding the remaining two equatorial ligands, as shown in Figs. 7 and 8.

An analysis of the copper binding site of human and chicken prion protein at pH 6.5 was performed by Redecke et al. (2005). The Cu^{2+} coordination of the octapeptide sequences of hPrP was studied by means of EXAFS using synthetic one, three and four successive copies of the octapeptide sequence. The Cu^{2+} concentration was chosen so that only 0.5 Cu^{2+} ions per binding site were available. The EXAFS spectrum of one octapeptide/Cu^{2+} complex at pH 6.5 differs from our measurement of the same complex at pH 7.15 (compare especially the peak at $k = 6.5$ Å^{-1} in their paper). It probably reflects the pH dependence. The EXAFS spectra of the tetraoctapeptide with two Cu^{2+} equivalents at pH 6.5 are different to our EXAFS measurements of the hPrP-[23-231] at pH 6.0 and pH 7.0 especially where one can find characteristic contributions of the imidazole coordination. The Cu^{2+} environment of the tetraoctapeptide is not necessarily the same as in hPrP-[23-231]. Moreover, it is known from the literature (Aronoff-Spencer et al. 2000) that the tetraoctapeptide binds Cu^{2+} at pH 6.5 with two different configurations. It is possible that the EXAFS spectra of (Redecke et al. 2005) are the result of samples with more than one Cu^{2+} species.

Recently Chattopadhyay et al. (2005) have published a study based on a variety of EPR techniques. Synthetic tetraoctapeptides were investigated at pH 7.4 with the attached sequence 23-28 of hPrP to increase solubility. The Cu^{2+} concentration ranged from 0.25 to 6 Cu^{2+} equivalents. They found two to three distinct EPR species present at the same time in a sample. At Cu^{2+} occupancies above 2.0 equivalents a component 1 dominated with parameters similar to our species I. A residual component 2 was found. At low Cu^{2+} occupancy, from 0.25 to 2 Cu^{2+} equivalents they found the component 2 and another component 3 with parameters similar to our species II. Component 1 is interpreted as 3N–1O complex in agreement with our species I. In the model proposed for component 2 two copper ions are bound in the octarepeat region: the copper complex is ligated by the N_δ of one imidazole ring, the deprotonated backbone nitrogen of the same histidine and two water molecules. The weakly bound fifth axial ligand is a nitrogen of another imidazole. In component 3 it is assumed that the Cu^{2+} is coordinated by three N atoms of histidines and a water oxygen (which could also be a nitrogen atom of a fourth histidine).

For a comparison with our model one has to bear in mind that our investigation were performed on a recombinant hPrP-[23-231]. We succeeded in the preparation of samples with defined species, either I or II. With respect to component 1 (our species I) our models are identical. Although our species II shows nearly the same EPR parameters as component 3, the model proposed by Chattopadhyay et al. (2005) for component 3 cannot explain our experimental findings concerning species II for hPrP-[23-231]: in our model we have two Cu^{2+} ions per tetraoctapeptide.

Although we could not determine a species corresponding to component 2 we tried to adopt their model for an interpretation of species II (see electronic supplementary material S4). We did this because the model for component 2 explains the binding of two Cu^{2+} ions per tetra octapeptide. We created models with the information given by Chattopadhyay et al. (2005). XPLOR and its simulated annealing protocols were used to calculate models. However, the EXAFS spectra calculated from this model were in clear disagreement with our experimental data because of the fifth ligand, the axially bound imidazole ring. In this comparison one should not forget that the model for component 2 was developed for a quite different sample.

The investigations presented here show the importance of the application of different experimental methods to resolve ambiguity in the individual results. Moreover, the extensive use of MD simulations allows to obtain structures with low energies and correct covalent geometry avoiding, e.g., improper bond lengths and angles. The simulated spectra of the calculated structures fully agree with the experimental data obtained by EPR, ENDOR, and EXAFS resulting in a reliable model for the Cu^{2+} complex of the octarepeat region in full-length $hPrP^C$. Our complex model differs significantly from those previously obtained for shorter peptides. Sequence context, buffer conditions and stoichiometry of copper show marked influence on the configuration of copper binding to PrP^C. It is

generally accepted that for an understanding of the function of a protein the knowledge of its structure is of highest value. Often the function can immediately be understood from the structure. Unfortunately, here this is not the case. In this context it may be of interest that we were unable to load the full-length PrP with four Cu-equivalents. There was, however, no problem to have this load in protein fragments like the tetra-octarepeat. Future studies will have to investigate whether different configurations are associated with different functional states of PrP^{C}.

Acknowledgments We are indebted to Elisabeth Weyher-Stingl and Brigitte Kraft for expert technical assistance. Help and advice on sample preparation from Prof. Shou-Liang Dong, Lanzhou University, China, during his visit at the MPI in Martinsried is gratefully acknowledged. This work was supported by the Bavarian government (FORPRION, grant LMU02).

References

Arnesano F, Banci L, Bertini I, Felli IC, Luchinat C, Thompsett AR (2003a) A strategy for the NMR characterization of type II copper(II) proteins: the case of the copper trafficking protein CopC from Pseudomonas Syringae. J Am Chem Soc 125:7200–7208

Arnesano F, Banci L, Bertini I, Mangani S, Thompsett AR (2003b) A redox switch in CopC: an intriguing copper trafficking protein that binds copper (I) and copper (II) at different sites. PNAS 100:3814–3819

Aronoff-Spencer E, Burns CS, Avdievich NI, Gerfen GJ, Peisach J, Antholine WE, Ball HL, Cohen FE, Prusiner SB, Millhauser GL (2000) Identification of the Cu^{2+} binding sites in the N-terminal domain of the prion protein by EPR and CD spectroscopy. Biochemistry 39:13760–13771

Binsted N, Strange RW, Hasnain SS (1992) Constrained and restrained refinement in EXAFS data analysis with curved-wave theory. Biochemistry 31:12117–12125

Brown DR, Qin K, Herms JW, Madlung A, Manson J, Strome R, Fraser PE, Kruck T, Bohlen Av, Schulz-Schaeffer W, Giese A, Westaway D, Kretzschmar H (1997) The cellular prion protein binds copper in vivo. Nature 390:684–687

Brünger AT (1992) X-PLOR version 3.1. The Howard Hughes Medical Institute, Department of Molecular Biophysics and Biochemistry

Brünger AT, Campbell RL, Clore GM, Gronenborn AM, Karplus M, Petsko GA, Teeter MM (1987) Solution of a protein crystal structure with a model obtained from NMR interproton distance restraints. Science 235:1049–1053

Burns CS, Aronoff-Spencer E, Dunham CM, Lario P, Avdievich NI, Antholine WE, Olmstead MM, Vrielink A, Gerfen GJ, Peisach J, Scott WF, Millhauser GL (2002) Molecular features of the copper binding sites in the octarepeat domain of the prion protein. Biochemistry 41:3991–4001

Burns CS, Aronoff-Spencer E, Legname G, Prusiner SB, Antholine WE, Gerfen GJ, Peisach J, Millhauser GL (2003) Copper coordination in the full-length, recombinant prion protein. Biochemistry 42:6794–6803

Chattopadhyay M, Walter ED, Newell DJ, Jackson PJ, Aronoff-Spencer E, Peisach J, Gerfen GJ, Benett B, Antholine WE, Millhauser GL (2005) The octarepeat domain of the prion proteins binds Cu(II) with three distinct coordination modes at pH 7.4. J Am Chem Soc 127:12647–12656

Frisch MJT, Schlegel GW, Scuseria HB, Robb GE, Cheeseman MA, Zakrzewski JR, Montgomery VG, Stratmann JA Jr, Burant RE, JC et al (1998) Gaussian 98. Gaussian Inc., Pittsburgh, PA

Giese A, Levin J, Bertsch U, Kretzschmar H (2004) Effect of metal ions on de novo aggregation of full-length prion protein. Biochem Biophys Res Commun 320:1240–1246

Hasnain SS, Murphy LM, Strange RW, Grossmann JG, Clarke AR, Jackson GS, Collinge J (2001) XAFS study of the high-affinity copper-binding site of human PrP^{91-231} and its low-resolution structure in solution. J Mol Biol 311:467–473

Herms J, Tings T, Gall S, Madlung A, Giese A, Siebert H, Schürmann P, Windl O, Brose N, Kretzschmar H (1999) Evidence of presynaptic location and function of the prion protein. J Neurosci 19:8866–8875

Hurst GC, Henderson TA, Kreilick RW (1985) Angle-selected ENDOR spectroscopy. 1. Theoretical interpretation of ENDOR shifts from randomly orientated transition-metal complexes. J Am Chem Soc 107:7294–7299

Katterle B, Gvozdev RI, Abudu N, Ljones T, Andersson KK (2002) A continuous-wave electron-nuclear double resonance (X-band) study of the Cu^{2+} sites of particulate methane mono-oxygenase of *Methylococcus capsulatus* (strain M) in membrane and pure dopamine β-mono-oxygenase of the adrenal medulla. Biochem J 363:677–686

Kramer ML, Kratzin HD, Schmidt B, Römer A, Windl O, Liemann S, Hornemann S, Kretzschmar H (2001) Prion protein binds copper within the physiological concentration range. J Biol Chem 276:16711–16719

Kretzschmar H, Prusiner S, Stowring L, DeArmond S (1986) Scrapie prion proteins are synthesized in neurons. Am J Pathol 122:1–5

Lemos SS, Collins MLP, Eaton SS, Eaton GR, Antholine WE (2000) Comparison of EPR-visible Cu^{2+} sites in pMMO from *Methylococcus capsulatus* (Bath) and *Methylomicrobium album* BG8. Biophys J 79:1085–1094

MacKerell AD Jr, Bashford D, Bellott M, Dunbrack RL Jr, Evanseck J, Field MJ, Fischer S, Gao J, Guo H, Ha S, Joseph D, Kuchnir L, Kuczera K, Lau FTK, Mattos C, Michnick S, Ngo T, Nguyen DT, Prodhom B, Reiher IWE, Roux B, Schlenkrich M, Smith J, Stote R, Straub J, Watanabe M, Wiorkiewicz-Kuczera JYD, Karplus M (1998) All-atom empirical potential for molecular modeling and dynamics studies of proteins. J Phys Chem 102:3586–3616

Mentler M, Weiss A, Grantner K, Del Pino P, Deluca D, Fiori S, Renner C, Meyer-Klaucke W, Moroder L, Bertsch U, Kretzschmar HA, Tavan P, Parak FG (2005) A new method to determine the structure of the metal environment in metalloproteins: investigation of the prion octapeptide repeat Cu^{2+}-complex. Eur Biophys J 34:97–112

Miura T, Hori-i A, Takeuchi H (1996) Metal-dependent alpha-helix formation promoted by the glycine-rich octapeptide region of prion protein. FEBS Lett 396:248–252

Miura T, Hori-i A, Mototani H, Takeuchi H (1999) Raman spectroscopic study on the copper(II) binding mode of prion octapeptide and its pH dependence. Biochemistry 38:11560–11569

Miura T, Sasaki S, Toyama A, Takeuchi H (2005) Copper reduction by the octapeptide repeat region of prion protein: pH dependence and implications in cellular copper uptake. Biochemistry 44:8712–8720

Morante S, González-Iglesias R, Potrich C, Meneghini C, Meyer-Klaucke W, Menestrina G, Gasset M (2004) Inter- and intra-octarepeat Cu(II) site geometries in the prion protein:

implications in Cu(II) binding cooperativity and Cu(II)-mediated assemblies. J Biol Chem 279:11753–11759
Moser M, Colello RJ, Pott U, Oesch B (1995) Developmental expression of the prion protein gene in glial cells. Neuron 14:509–517
Nicholl D, Windl O, de Silva R, Sawcer S, Dempster JW (1995) Inherited Creutzfeldt-Jakob disease in a British family associated with a novel 144 base pair insertion of the prion protein gene. J Neurol Neurosurg Psychiatry 58:65–69
Nolting HF, Hermes C (1992) EXPROG: EMBL EXAFS data analysis package for PC/AT
Pauly PC, Harris DA (1988) Copper stimulates endocytosis of the prion protein. J Biol Chem 273:33107–33110
Peisach J, Blumberg WE (1974) Structural implications derived from the analysis of electron paramagnetic resonance spectra of natural and artificial copper proteins. Arch Biochem Biophys 165:691–708
Pettifer RF, Hermes C (1985) Absolute energy calibration of X-ray radiation from synchrotron sources. J Appl Crystallogr 18:404–412
Prusiner SB (1998) Prions. Proc Natl Acad Sci USA 95:13363–13383
Redecke L, Meyer-Klaucke W, Koker M, Clos J, Georgieva D, Genov N, Echner H, Kalbacher H, Perbandt M, Bredehorst R, Voelter W, Betzel C (2005) Comparative analysis of the human and chicken prion protein copper binding regions at pH 6.5. J Biol Chem 14:13987–13992
Rehr JJ, Albers RC (1990) Scattering-matrix formulation of curved-wave multiple-scattering theory: application to X-ray-absorption fine structure. Phys Rev B 41:8139–8149
Renner C, Fiori S, Fiorino F, Landgraf D, Deluca D, Mentler M, Grantner K, Parak FG, Kretzschmar H, Moroder L (2004) Micellar environments induce structuring of the N-terminal tail of the prion protein. Biopolymers 73:421–433
Scholl H-J, Hüttermann J (1992) ESR and ENDOR of Cu(II) complexes with nitrogen donors: probing parameters for prosthetic group modeling of superoxide dismutase. J Phys Chem 96:9684–9691
Skworc KH, Windl O, Schulz-Schaeffer WJ, Giese A, Bergk J, Nägele A, Vieregge P, Zerr I, Poser S, Kretzschmar HA (1999) Familial Creutzfeldt-Jakob disease with a novel 120-bp insertion in the prion protein gene. Ann Neurol 46:693–700
Stahl N, Borchelt DR, Hsiao K, Prusiner SB (1987) Scrapie prion protein conatinas a phosphatidylinositol glycolipid. Cell 51:229–240
Stöckel J, Safar J, Wallace AC, Cohen FE, Prusiner SB (1998) Prion protein selectively binds copper(II) ions. Biochemistry 37:7185–7193
Van Doorslaer S, Cereghetti GM, Glockshuber R, Schweiger A (2001) Unraveling the Cu^{2+} binding sites in the C-terminal domain of the murine prion protein: a pulse EPR and ENDOR study. J Phys Chem B 105:1631–1639
Viles JH, Cohen FE, Prusiner SB, Goodin DB, Wright PE (1999) Copper binding to the prion protein: structural implications of four identical cooperative binding sites. Proc Natl Acad Sci USA 96:2042–2047
Windl O, Dempster M, Estibeiro JP, Lathe R, de Silva R, Esmonde T, Will R, Springbett A, Campbell TA, Sidle KC, Palmer MS, Collinge J (1996) Genetic basis of Creutzfeld-Jakob disease in the United Kingdom: a systematic analysis of predisposing mutations and allelic variation in the PRNP gene. Hum Genet 98:259–264
Yuan H, Collins MLP, Antholine WE (1999) Type 2 Cu^{2+} in pMMO from *Methylomicrobium album* BG8. Biophys J 76:2223–2229